

Pivotal Role of Tibetan Plateau and Antarctic in Shaping Present-day Atlantic Meridional Overturning Circulation

Mingjun Tong^a, Haijun Yang^{*a}, Rui Jiang^b, and Peili Wu^c

^a*Department of Atmospheric and Oceanic Sciences and Key Laboratory of Polar Atmosphere-ocean-ice System for Weather and Climate of Ministry of Education, Fudan University, Shanghai, 200438, China*

^b*Department of Atmospheric and Oceanic Sciences, School of Physics, Peking University, Beijing, 100871, China*

^c*Met Office Hadley Centre, UK*

Journal of Climate

1st submission: May 30, 2024

1st revision: September 8, 2024

2nd revision: December 11, 2024

**Corresponding author address:* Haijun Yang, Department of Atmospheric and Oceanic Sciences, Fudan University, 2005 Songhu Road, Shanghai, 200438, China.

Email: yanghj@fudan.edu.cn

20

ABSTRACT

21

22

23

24

25

26

27

28

29

30

31

32

33

34

35

36

Our recent study has shown key roles of the Tibetan Plateau and Antarctic orography in the formation of the Atlantic Meridional Overturning Circulation (AMOC). This is a follow-up investigation to elucidate physical processes of the combined effect by comparing two different sets of experiments: starting from a global flat orography, one to incorporate the Tibetan Plateau (TP) first followed by the Antarctica (TP2AT) and the other to introduce the Antarctica first followed by the TP (AT2TP). The uplift of the TP significantly modifies moisture transport in the Northern Hemisphere, leading to a fresher North Pacific and a more saline North Atlantic. This alteration of atmospheric moisture transport is essential for the transition of deep-water formation from the North Pacific to the North Atlantic, which activates the AMOC. The role of Antarctic orography is mainly associated with its influence on the atmospheric westerlies over the subpolar Southern Hemisphere, which can strengthen the AMOC by boosting Ekman pumping and Agulhas leakage in the Southern Ocean. The combined influence of the TP and the Antarctica is the key driving factor for establishing the current configuration of the AMOC. The sequence of the TP going before the Antarctica (TP2AT) is more effective in setting up the AMOC than the other way around (AT2TP). This is because in AT2TP it takes time to terminate a strong Pacific Meridional Overturning Circulation (PMOC) before the AMOC gets into a full swing.

37

KEYWORDS: Atlantic Meridional Overturning Circulation, Pacific Meridional Overturning

38

Circulation, Tibetan Plateau, Antarctica, Coupled Model

39 **1. Introduction**

40 The Atlantic Meridional Overturning Circulation (AMOC) is a crucial part of the present-day
41 global climate system. Its fluctuations and potential responses to ongoing global warming are a global
42 concern. The AMOC is also considered to hold a tipping point within the climate system (van Westen
43 et al. 2024). Both observational data and model simulations have indicated a weakening AMOC
44 during the recent period and the consequent accumulation of salinity in the South Atlantic (Zhu and
45 Liu 2020). Some model projections suggested that this weakening trend of the AMOC may persist
46 over the coming decades due to ongoing freshwater influx from the melting of Greenland's ice sheets
47 (Weijer et al. 2012). Some researchers even suggested that a transition of the AMOC could happen as
48 early as 2025 (Ditlevson and Ditlevson 2023). The future of the AMOC remains a hot topic in climate
49 research.

50 To assess potential future changes of the AMOC, it is essential to understand the fundamental
51 factors driving it. Traditional views of the AMOC are that it is maintained by buoyancy forcing in the
52 North Atlantic and by wind stress forcing over the Southern Ocean (Johnson et al. 2019; Bryden
53 2021). The significance of large continental orography, such as massive mountain ranges, in shaping
54 the modern-day AMOC has also been increasingly recognized (Sinha et al. 2012; Maffre et al. 2018;
55 Yang and Wen 2020; Jiang and Yang 2021; Schmittner et al. 2011; Stouffer et al. 2022). Numerous
56 simulations suggested that on a hypothetical Earth without significant topographical relief, the Pacific
57 Meridional Overturning Circulation (PMOC) would predominate rather than the AMOC (Sinha et al.,
58 2012). If all the giant mountains are removed, the modern-day MOC would be switched from the
59 Atlantic to the Pacific (Maffre et al. 2018). In today's world there is no deep-water formation in the
60 North Pacific, primarily because the surface seawater in that ocean basin is not dense enough to sink.

61 Geological evidence indicates that the uplift of the Tibetan Plateau (TP), the highest plateau in the
62 world, coincides with the formation of the North Atlantic Deep Water (NADW), illustrating a
63 potential role of the TP in shaping the AMOC (Ivanova 2009; Ferreira et al. 2018; Yang and Wen
64 2020; Liu et al. 2022). The significant elevation of the TP can dramatically impact the mid-latitude
65 westerlies, thereby altering moisture transport patterns (Liu et al. 2007; Tang et al. 2022). These
66 changes can profoundly influence buoyancy-driven thermohaline circulations (Yang and Wen 2020).
67 Previously, we conducted a series of orography sensitivity experiments using coupled models,
68 focusing on the impact of continental orography on the global meridional overturning circulation
69 (GMOC) (Yang et al. 2024). Our findings show that the rise of the TP is indispensable in the

70 formation of the AMOC. However, the TP alone is insufficient to fully establish the AMOC, which
71 requires the contribution of other significant orography. Specifically, only the Antarctic has the
72 capability to complement the TP's influence and achieve the complete establishment of the AMOC, as
73 we will demonstrate in this paper.

74 Polar regions are sensitive to changes in the climate system; and the interactions between polar
75 regions and ocean circulations may potentially trigger cascading effects on global climate (Dekker et
76 al. 2018). Around three million years ago (Ma), the expansion of the Antarctic ice-sheets initiated
77 changes in deep ocean circulation, hastening glaciation in the Northern Hemisphere (Woodard et al.
78 2014). Wind-induced upwelling process in the Southern Ocean can drive the AMOC (Kuhlbrodt et al.
79 2007). A strong meridional gradient in the westerlies over the Southern Ocean can significantly
80 enhance the upwelling of deep-water masses and thus strengthen the NADW formation (Delworth
81 and Zeng 2008). Additionally, a warmer Southern Ocean is usually linked to a stronger AMOC
82 through a reduction in the formation of the Antarctic Bottom Water (AABW) and strengthening of the
83 Agulhas leakage (Buizert and Schmittner 2015). Despite the recognized importance of physical
84 processes in the Southern Ocean for the AMOC, research focusing specifically on Antarctica's impact
85 on the AMOC is limited.

86 Researchers have long acknowledged that the influence of continental orography on modern-day
87 ocean circulations. Prior investigations typically concentrated on understanding how the presence or
88 absence of global mountain ranges impacts ocean currents and on isolating the influence of individual
89 topography. Sinha et al. (2012) and Maffre et al. (2018) concluded the global large orography's
90 importance on shaping modern-day MOC. Both of these studies emphasized that mountains matter in
91 changing the heat and freshwater fluxes over the ocean, thus altering the ocean circulation mode.
92 Maffre et al. (2018) argued that Rocky Mountain is critical to shift the area of strong precipitation and
93 change the river runoff towards the tropical Atlantic, which leads to the change of AMOC. These
94 conclusions are consistent with Schmittner et al. (2011)'s work, who argued that the existence of the
95 Andes and the Rocky Mountains reduce atmospheric moisture transport from the Pacific to the
96 Atlantic. So, the North Atlantic becomes saltier and the North Pacific becomes fresher. However, as
97 the whole continental orography is removed in the above studies, it is hard to conclude the reason for
98 the MOC shift being caused by mountains in North America. Maroon (2016) utilized the Geophysical
99 Fluid Dynamics Laboratory (GFDL) model and revealed a significant enhancement of the PMOC in a
100 removing-Rocky experiment. However, this change was not attributed to the traditionally assumed

101 influence on the wind field (Maffre et al. 2018; Sinha et al. 2012), but rather to the effect of river
102 runoff. Furthermore, it was found that keeping the Rocky Mountain while altering the direction of
103 river runoff would also modify the MOC pattern. A previous work in our research group conducted
104 Rocky Mountain-only experiment and found that Rocky Mountain's existence has a weak effect on
105 AMOC (Jiang and Yang. 2021). Since the locations of deep-water formation and variations in river
106 runoff differ across models, the role of the Rocky Mountains in influencing the MOC remains a
107 subject of ongoing debate. Yang et al. (2024; hereafter Y24) then conducted a brief examination of
108 the collective impact of different mountainous regions on the GMOC. Their findings suggested that
109 the TP and Antarctica, through their respective influences on deep-water formation and Ekman
110 pumping, can jointly facilitate a complete establishment of the AMOC. Building upon the
111 groundwork laid by Y24, this paper aims to investigate detailed processes translating the synergistic
112 effects of the TP and the Antarctic into the establishment of the AMOC.

113 This paper is organized as follows. In Section 2, we present the models and experiments used in
114 this study. In Section 3, we detail the changes in the AMOC resulting from the uplift of the TP and
115 Antarctica orography, in different orders. The mechanisms underlying the combined effects of the TP
116 and Antarctica on the AMOC are thoroughly investigated in Section 4. A summary of our findings is
117 presented in Section 5, together with a discussion on their implications.

118

119 **2. Model and experiments**

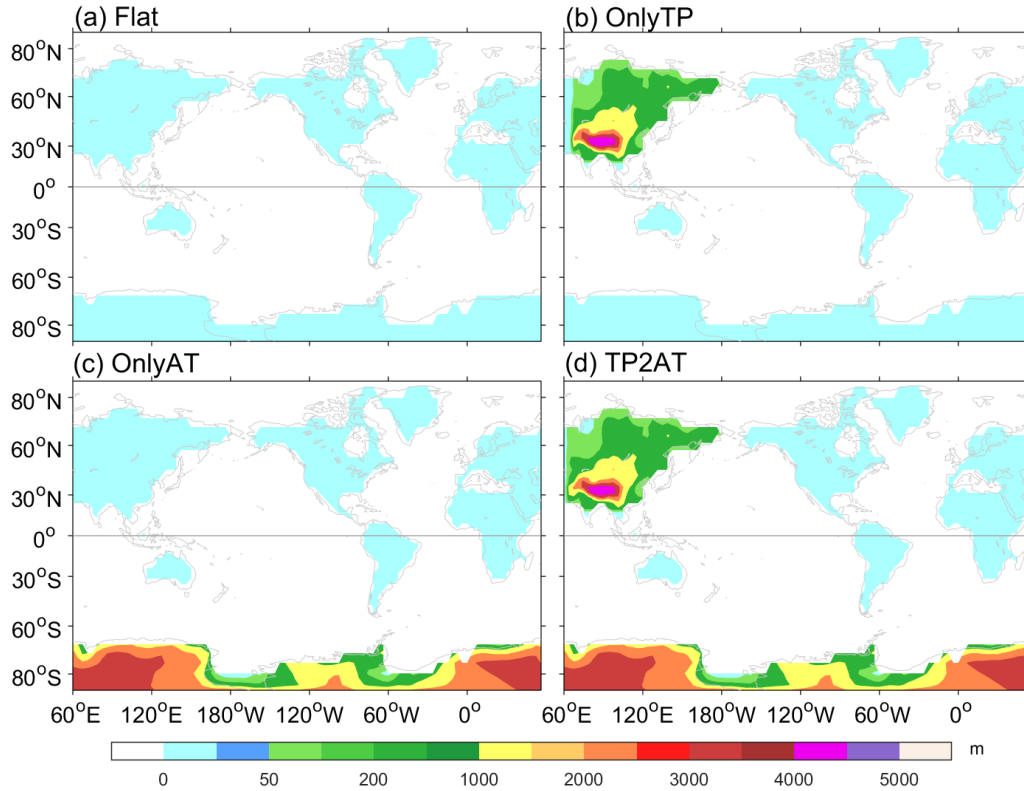
120 The Community Earth System Model (CESM) is developed by the United States' National Center
121 for Atmospheric Research (NCAR) and the climate research community. It is a fully coupled climate
122 model that enables simulations of the past, present, and future climate of the Earth. It is widely used
123 in examining atmospheric processes, ocean circulations, and the interactions between them. The
124 model comprises six components: atmosphere, land, ocean, sea ice, land ice, and a coupler. The
125 CESM version 1.0.4 is employed in this study, with a resolution of T31_gx3v7. Specifically, the
126 CAM4 is the atmospheric module, and the POP2 is the oceanic module. The atmosphere and land
127 models have 48 and 96 grid points in the horizontal direction with a resolution of
128 approximately $3.75^\circ \times 3.75^\circ$, and the atmosphere has 26 vertical levels. The ocean model POP2
129 employs the gx3v7 grid, with a uniform zonal grid spacing of 3.6° and non-uniform meridional grid.
130 The meridional resolution is 3.4° around 35°N and 35°S , and gradually increases towards the equator

131 and poles, reaching 0.6° near the equator. The ocean has 60 vertical layers. The horizontal resolution
132 of the sea ice model is the same as that of the ocean model. Further details on CESM1.0 can be found
133 in Hurrell et al. (2013).

134 Some experiments analyzed in this paper were performed previously (see Y24), including the
135 “Real,” “Flat,” “OnlyTP,” and “OnlyAT” simulations. The “Real” simulation incorporates realistic
136 terrestrial topography; it was run for 2400 years, serving as a benchmark for comparing the effects of
137 topography on ocean circulations. Conversely, the “Flat” simulation assumes an Earth with a uniform
138 altitude of 10 meters above sea level globally; it was integrated for 1600 years (Fig. 1a). The
139 simulations “OnlyTP” (Fig. 1b) and “OnlyAT” (Fig. 1c) modify the “Flat” scenario by incorporating
140 the topography of the TP and Antarctica, respectively. These two experiments, designed to isolate the
141 effects of individual topographies, were run for 1600 years each, starting from year 801 of the “Flat”
142 simulation.

143 To explore the combined influence of the TP and Antarctica on the AMOC, we use two distinct
144 sets of topographical experiments: “TP2AT” and “AT2TP.” The “TP2AT” experiment involves
145 adding Antarctic terrain to the “OnlyTP” setup, and is integrated for an additional 2400 years starting
146 from year 2401 of the “OnlyTP” run (Fig. 1d). The “AT2TP” experiment introduces the TP into the
147 “OnlyAT” scenario, and is integrated for the same duration as “TP2AT.” The primary distinction
148 between “TP2AT” and “AT2TP” lies in the sequence in which the terrains are incorporated. Our
149 analysis focus on the quasi-equilibrium stages of these experiments using annual mean fields: model
150 years 801-1200 for “Flat,” years 2001-2400 for the individual terrain experiments, and years 4401-
151 4800 for the combined terrain experiments of TP2AT” and “AT2TP.”

152 All experiments use the same boundary conditions except for topographical height. The
153 geographical setup reflects modern-day conditions, without adjustments for plate tectonic movements.
154 Atmospheric CO_2 level is kept constant at the preindustrial level (285 ppm); and the model does not
155 account for changes in river routes or vegetation types. Continental ice sheets are represented as inert
156 “bright rocks” within the model, allowing planetary albedo to self-adjust according to changing
157 thermal conditions. Annual mean model outputs are used for analysis.



158

159 FIG. 1. Topography configuration in coupled model experiments. (a) Modified topography with flat global
 160 topography used in Flat, (b) modified topography with the inclusion of the Tibetan Plateau (TP) used in
 161 OnlyTP, (c) modified topography with the inclusion of Antarctic (AT) topography used in OnlyAT, and (d)
 162 modified topography with the TP and AT used in TP2AT and AT2TP. Shading represents surface geopotential
 163 heights (units: m)

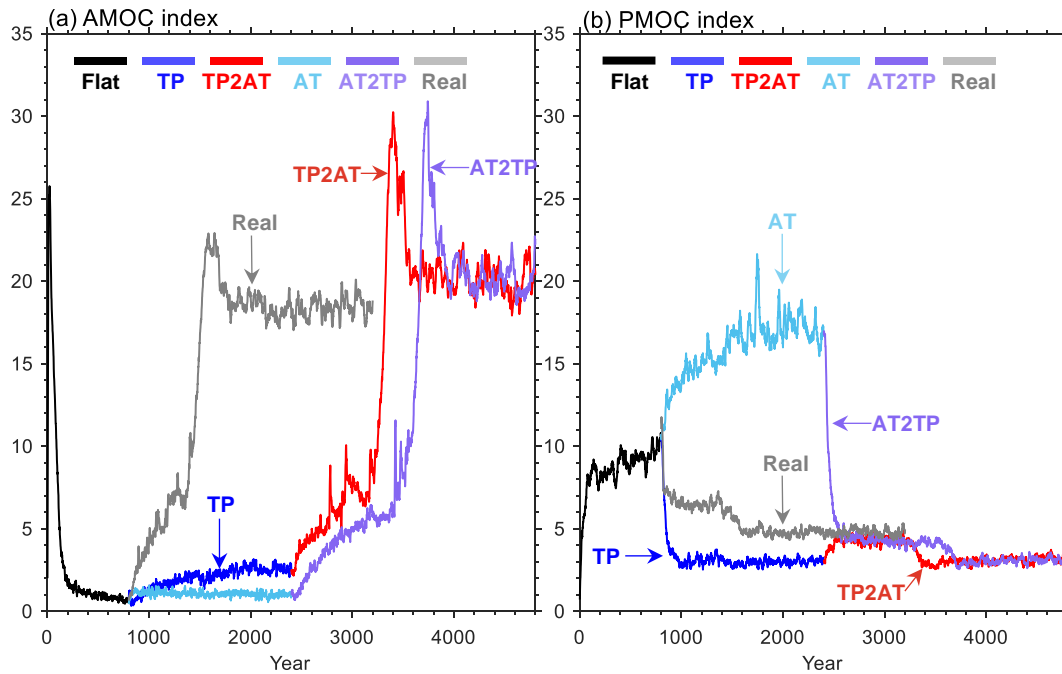
164

165 When examining the combining influence of the TP and Antarctica, the contribution of the TP can
 166 be discerned by using AT2TP minus OnlyAT; and that of the Antarctica, by using TP2AT minus
 167 OnlyTP. The individual roles of the TP and Antarctica can be obtained by comparing OnlyTP with
 168 Flat and by comparing OnlyAT with Flat, respectively. Note that some experiments exhibit an initial
 169 adjustment marked by a sudden jump in variables when topography is introduced abruptly. These
 170 initial fluctuations have minimal effects on the quasi-equilibrium state.

171

172 **3. Effects of the TP and Antarctica on meridional overturning circulation**

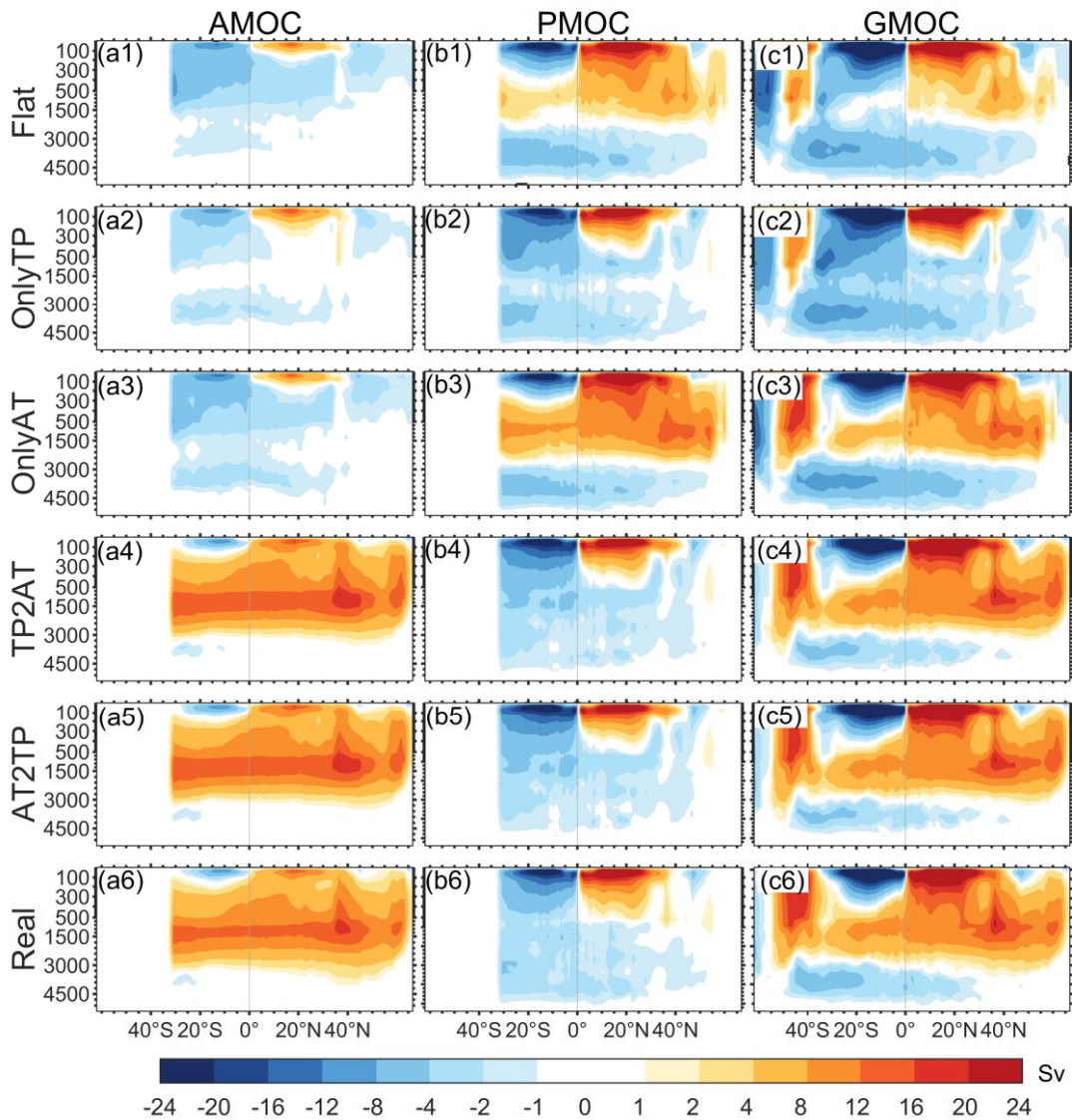
173 Previous studies reached a consensus that current mountains on the Earth matter in the formation
 174 of the AMOC, of which the TP matters the most and the Antarctic plays as a secondary role (Y24).
 175 This can also be seen in the evolutions of the AMOC and PMOC indices in TP2AT and AT2TP
 176 clearly (Fig. 2). In TP2AT, the AMOC reaches its peak value by the 3400th year, approximately 1000
 177 years after the introduction of the Antarctic orography. However, this maturation process takes
 178 several hundred years longer in the AT2TP scenario (Fig. 2a). The basic idea is that the uplift of the
 179 TP in TP2AT immediately leads to anomalous atmospheric moisture transport from the North
 180 Atlantic to the North Pacific, shutting down the PMOC quickly (Fig. 2b) and initializing the NADW
 181 formation. The introduction of the Antarctic orography subsequently supports the NADW formation
 182 by enhancing Ekman pumping in the Southern Ocean. In AT2TP, the PMOC is bolstered due to
 183 increased Ekman pumping in the Southern Ocean in response to the Antarctic orography. The uplift
 184 of the TP has to first counteract this enhanced PMOC before it can begin the process of the NADW
 185 formation. The specifics of these processes will be discussed in Section 4.



186
 187 FIG. 2. Temporal evolutions of (a) the Atlantic meridional overturning circulation (AMOC) and (b) Pacific
 188 meridional overturning circulation (PMOC) in different topography experiments (units: Sv; $1\text{ Sv} = 10^6 \text{ m}^3\text{s}^{-1}$).
 189 The AMOC index is defined as the maximum stream function at depths of 400-2000 m and $20^\circ\text{-}70^\circ\text{N}$ in the
 190 North Atlantic. The PMOC index is calculated similarly, except in the North Pacific. All the curves are
 191 smoothed by a 10-year running mean.

192

193 Spatial patterns of the AMOC, PMOC, and GMOC under four different scenarios are illustrated in
 194 Fig. 3. The presence of the TP suppresses thermohaline circulation in the Pacific (comparing Figs.
 195 3b2 and b1), while the Antarctic orography generally enhances thermohaline circulation. (Evident in
 196 the comparison between Figs. 3b1 and b3, and between Figs. 3a2 and a4). However, neither the TP or
 197 Antarctic orography alone can lead to the establishment of the AMOC (Figs. 3a2 and a3). It is
 198 established only through the presences of both TP and Antarctica. This is clearly seen in the similar
 199 patterns and strengths of the meridional overturning circulation across the TP2AT, AT2TP, and Real
 200 experiments (Figs. 3a4-c6), indicating that the orography of other continents does not significantly
 201 impact the formation of the AMOC. This underscores the unique and complementary roles of the TP
 202 and Antarctic orography in shaping the modern-day AMOC.



204 FIG. 3. Patterns of (a) the AMOC, (b) PMOC, and (c) GMOC in different experiments (units: Sv). The MOCs
205 are averaged over years 801-1200, 2001-2400, 4401-4800, and 2601-3000 in Flat, OnlyTP and OnlyAT,
206 TP2AT and AT2TP, and Real, respectively.

207

208 **4. Mechanisms behind the joint effect of the TP and Antarctica**

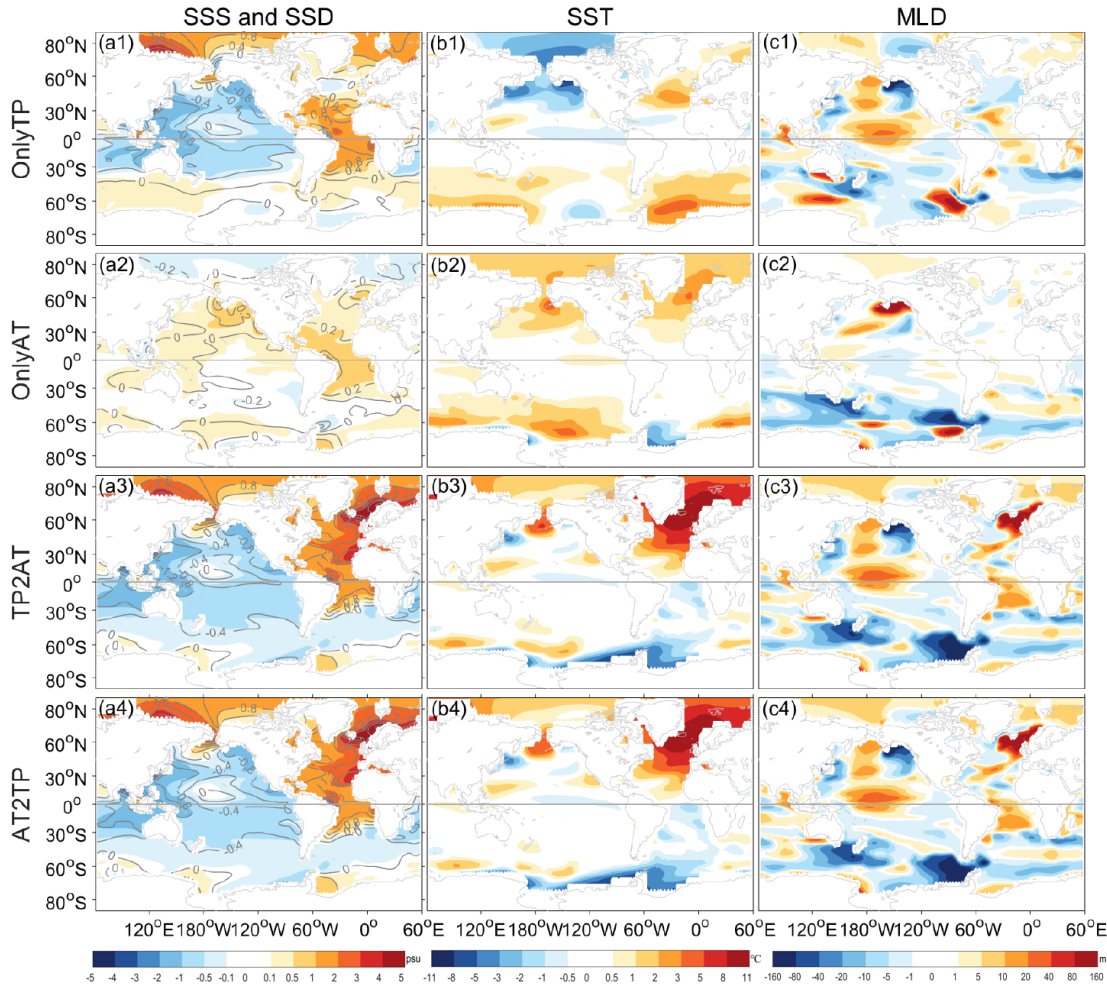
209 *a. Ocean buoyancy change*

210 The changes in buoyancy across the global surface ocean are shown in Fig. 4. The uplift of the TP
211 causes significant freshening in the North Pacific compared to the Flat scenario (Fig. 4a1), which is
212 the key factor leading to the shutdown of the PMOC. Concurrently, most areas of the Atlantic exhibit
213 surface salinization, with a mild freshening occurring in the NADW formation region. This mild
214 freshening prevents the establishment of the AMOC. It is observed that the change in sea-surface
215 salinity (SSS) predominantly influences the changes in sea-surface density (SSD), as illustrated in
216 Fig. 4a1. While the changes in sea-surface temperature (SST) shown in Fig. 4b1 tend to increase SSD,
217 they only slightly counterbalance the impact of SSS on SSD. The critical role of SSS in affecting
218 SSD, and thereby influencing deep-water formation in both North Pacific and North Atlantic, was
219 studied theoretically as early as in Stommel (1961). Additionally, geographical differences between
220 the Atlantic and Pacific basins affect salinity distribution, contributing to the Atlantic's stronger deep-
221 water formation compared to the Pacific (Ferreira et al. 2018; Yang and Wen 2020).

222 In the presence of Antarctic orography only, the SSS values in both Pacific and Atlantic are
223 increased slightly compared to those in the Flat scenario (Fig. 4a2), which apparently helps enhance
224 the PMOC in Flat. When the TP and Antarctic orography coexist, the surface freshening in the Pacific
225 is almost similar compared to that in OnlyTP (Figs. 4a3, a4), while in the Atlantic basin north of 30°S
226 the SSS increases significantly, which is particularly clear in the subtropical-subpolar North Atlantic.
227 This SSS change is critical to the establishment of the AMOC. Note that the subpolar North Atlantic
228 undergoes significant warming (Figs. 4b3 and b4), which is the consequence of the AMOC's
229 formation. Additionally, the buoyancy patterns in the TP2AT and AT2TP experiments are nearly
230 identical, suggesting that the climate system's quasi-equilibrium responses do not vary based on the
231 sequence of topographical introductions in our sensitivity experiments. This also indicates a
232 robustness in the climate system's reaction to these large-scale orographic features.

233 The changes in March mixed layer depth (MLD) (Fig. 4c) are consistent with the changes in the
234 deep-water formation region and thus the meridional overturning circulation. In OnlyTP, the MLDs in
235 both North Pacific and North Atlantic shoal, compared to that in the Flat scenario (Fig. 4c1),
236 consistent with the PMOC shutdown and the weak AMOC. In OnlyAT, the MLD is deepened in the
237 North Pacific (Fig. 4c2), consistent with the enhanced PMOC. In TP2AT and AT2TP, the MLD
238 changes are nearly identical, shoaling in the North Pacific and deepening in the North Atlantic (Figs.
239 4c3, c4), consistent with the PMOC shutdown and AMOC establishment.

240 Regarding the Pacific basin north of the equator, the changes in SSS, SSD, and MLD in OnlyTP
241 closely mirror those in TP2AT and AT2TP, suggesting that the TP alone has an important influence
242 on the ocean state across much of the Pacific, including both the wind-driven and thermohaline
243 circulations. The TP's impact in this region appears to be decisive and substantial. In contrast, when
244 considering the ocean state in the North Atlantic, the involvement of Antarctic orography becomes
245 necessary to complement the effects of the TP. The Antarctic's contribution is crucial for adjusting
246 the North Atlantic's conditions to facilitate the establishment of the AMOC. This interplay between
247 the TP and Antarctica highlights combined dynamics where the influence of one is enhanced or
248 modulated by the presence of the other, particularly in influencing the characteristics of global ocean
249 circulations and, by extension, the global climate system.



250

251 FIG. 4. Changes of (a) sea-surface salinity (SSS) (shading; units: psu) and sea-surface density (SSD) (contour;
 252 units: kg/m^3), (b) sea-surface temperature (SST) (units: $^{\circ}\text{C}$), and (c) March mixed layer depth (MLD) (units: m)
 253 in different experiments, with respect to Flat. March MLD represents the site of the deepest vertical mixing and
 254 convection, and thus deep-water formation, which is defined the same way as in Large et al. (1997).

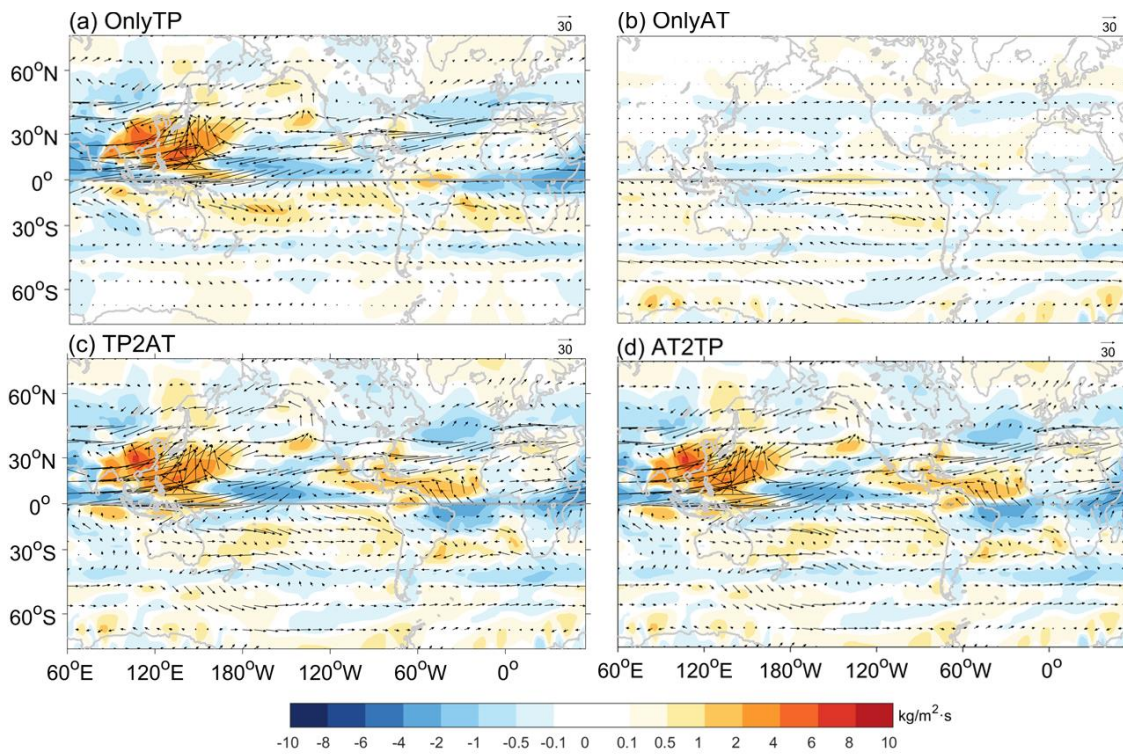
255

256 *b. Atmospheric moisture transport*

257 The SSS changes in the North Pacific and North Atlantic are largely caused by the net surface
 258 freshwater flux (i.e., evaporation minus precipitation, or EMP). This has been examined in details in
 259 similar sensitivity experiments of our previous study (Yang and Wen 2020). For a steady state, the
 260 EMP across the ocean surface is equivalent to the vertically integrated moisture transport divergence
 261 over the entire atmosphere column, when neglecting the freshwater flux on land surface and in river
 262 runoff (Jiang and Yang. 2021). Figure 5 shows the changes in moisture transport and convergence in

263 four different experiments, with respect to the Flat scenario. It is clear that the TP has significant
 264 effects on the global hydrological pattern in the Northern Hemisphere (Figs. 5a, c, d), while the effect
 265 of Antarctic orography on the Northern Hemisphere is negligible (Fig. 5b).

266 The uplift of the TP attracts a large amount of moisture from the Western Hemisphere, tropical
 267 Pacific, and Indian Ocean (Fig. 5a), which converges over East China and the western subtropical
 268 Pacific. The accumulation of freshwater in the western Pacific, coupled with its northward transport
 269 by the Kuroshio and subsequent eastward transport around 40°N by the Kuroshio Extension,
 270 ultimately leads to the shutdown of the PMOC. Similar processes were illustrated in Wen and Yang
 271 (2020). Concurrently, less freshwater converges in the North Atlantic surface due to the enhanced
 272 westward moisture transport across the ocean and North American continent. It is noteworthy that the
 273 moisture changes over the North Atlantic in OnlyTP are similar to those in TP2AT and AT2TP, in
 274 terms of both pattern and magnitude. This suggests that changes in surface freshwater flux alone are
 275 insufficient to induce strong NADW formation. In TP2AT and AT2TP, significant Ekman pumping
 276 occurs in the Southern Ocean, which serves an essential auxiliary role in the processes leading to the
 277 full establishment of the AMOC.



278

279 FIG. 5. Changes of vertically integrated moisture transport (vector; units: $\text{kg/m} \cdot \text{s}$) and moisture convergence
 280 (shading; units: $10^{-5} \text{ kg/m}^2 \cdot \text{s}$) in (a) OnlyTP, (b) OnlyAT, (c) TP2AT, and (d) AT2TP, with respect to Flat.

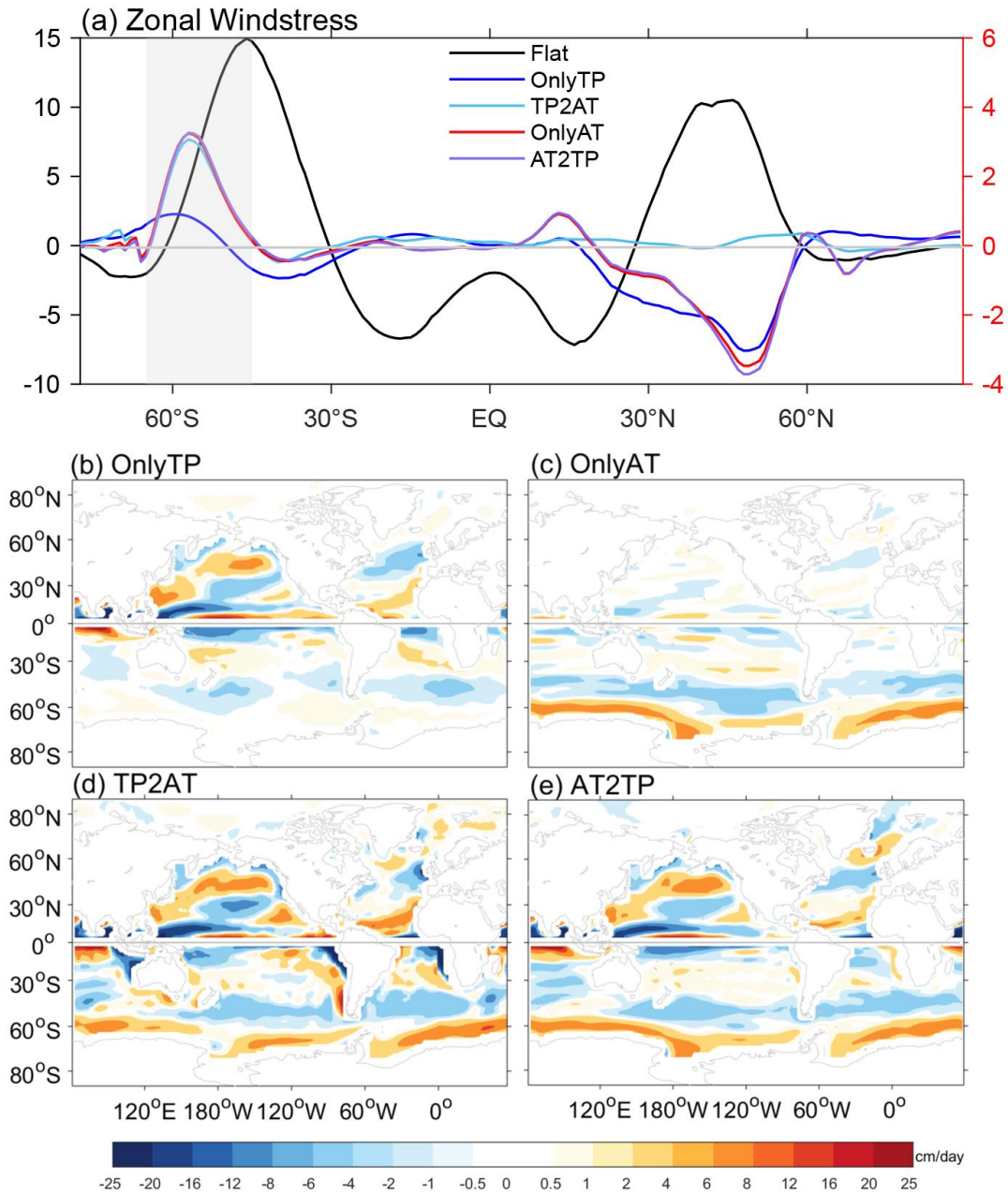
281 Positive value in moisture convergence represents the freshwater flux from atmosphere to ocean, i.e.,
282 freshwater gain by the ocean.

283

284 *c. Ekman pumping*

285 Indeed, the increase of freshwater in the North Pacific surface and the decrease in the North
286 Atlantic surface are primarily due to the weakening of mid-latitude westerlies (Fig. 6a), a response to
287 the TP's uplift. The TP's elevation also leads to significant Ekman upwelling in the North Pacific
288 (Figs. 6b, d, e), driven by changes in atmospheric circulations (figure not shown). This Ekman
289 pumping creates conditions favorable for shutting down the PMOC. Additionally, the weakened
290 westerlies result in reduced evaporation, contributing to the freshening of the North Pacific's surface
291 waters and to diminished vertical mixing in the region, which further weakens deep-water formation
292 in the North Pacific, thus playing a role in the PMOC's decline.

293



294

295 FIG. 6. (a) Mean westerlies in Flat (black curve; units: N/m^2 ; with the scale along the left ordinate) and its
 296 change in different experiments (with the scale along the right ordinate). Legends for curves are labeled. (b)-(e)
 297 Changes in Ekman pumping (units: cm/day) in OnlyTP, OnlyAT, TP2AT, and AT2TP, with respect to Flat,
 298 respectively. Positive (negative) value represents Ekman upwelling (downwelling).

299

300 Notable changes in Ekman pumping occur in the Southern Ocean along the Antarctic continent in
 301 AT, TP2AT, and AT2TP (Figs. 6c, d, e). The presence of the Antarctic orography results in stronger
 302 westerlies in the subpolar Southern Hemisphere compared to the Flat scenario (Fig. 6a), which in turn

303 drives robust Ekman pumping near the Antarctic continent (Figs. 6c, d, e). This Ekman pumping
304 induces a southward flow at depth while enhancing the northward Ekman flow at the surface, playing
305 a pivotal role in facilitating deep-water formation in the Northern Hemisphere, albeit remotely.

306 It is important to highlight that the specific location of deep-water formation is influenced by this
307 mechanism in different ways. In scenarios where deep-water formation occurs in the North Pacific,
308 such as in the Flat scenario, the Antarctic orography can augment the North Pacific Deep Water
309 (NPDW) formation, thereby enhancing the PMOC. Conversely, when deep-water formation takes
310 place in the North Atlantic, as seen in the scenarios involving the TP, the Antarctic orography can
311 boost the NADW formation, and thus the AMOC. The direction of the southward pumping in the
312 Southern Ocean, driven by the strong westerlies, does not inherently determine its source waters.

313

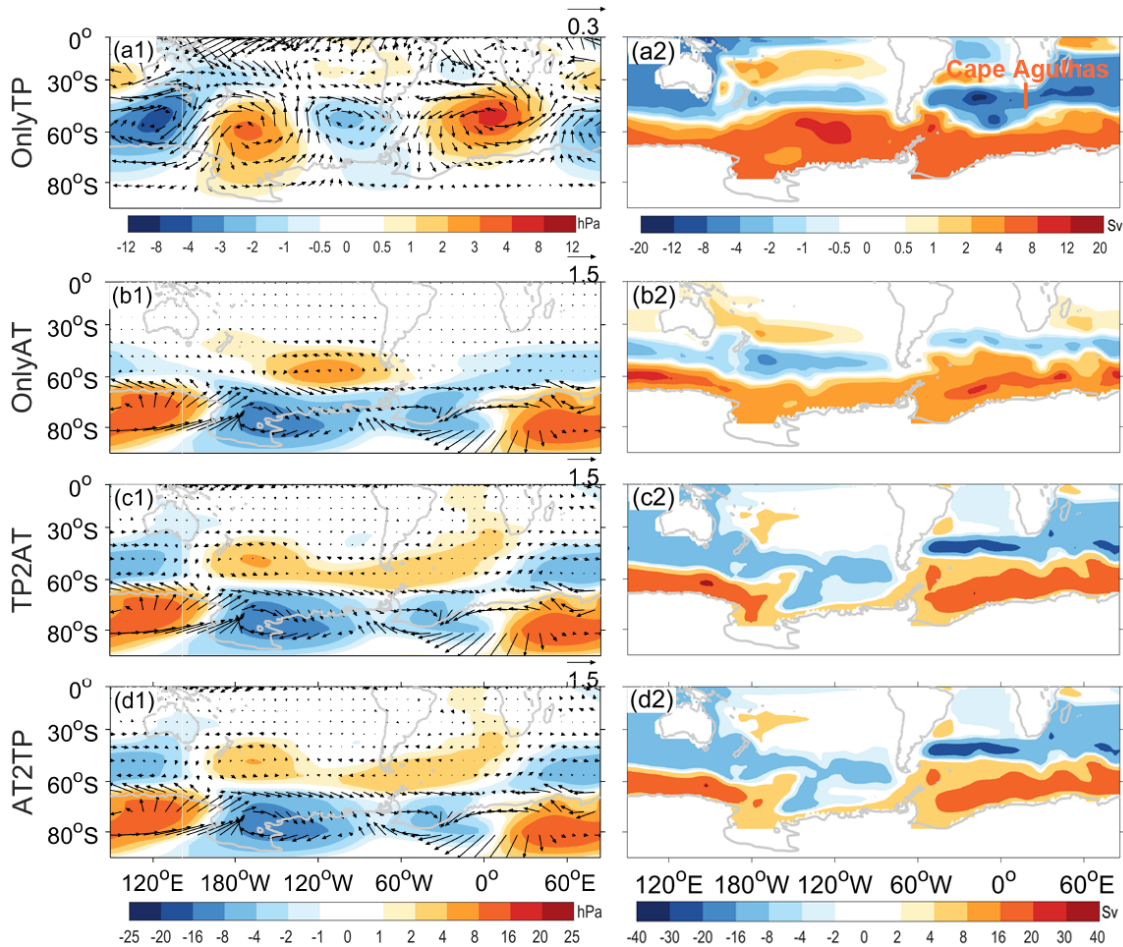
314 *d. Agulhas leakage and meridional mass transport*

315 When TP exist alone, it can affect the Southern Ocean through Rossby wave train (Fig. 7a1),
316 leading to a slight enhancement of the Antarctic circumpolar current (ACC) and the Agulhas leakage
317 (Fig. 7a2) in OnlyTP. The latter can contribute about 1~2 Sv water mass transport to the northward
318 upper warm route of the AMOC (Beal et al. 2011). The TP's far-reaching effects on the Southern
319 Ocean were revealed in Wang et al. (2023). The tropical Indian Ocean plays a role in the
320 teleconnection between the TP and Southern Ocean, which occurs mainly in the austral winter. An
321 anomalous high is generated to the south of Cape Agulhas in OnlyTP (Fig. 7a1), and the anomalous
322 easterlies near Cape Agulhas enhances the Agulhas leakage by about 2-3 Sv (Fig. 7a2). The Agulhas
323 Current is the western boundary current of the subtropical gyre in the southern Indian Ocean,
324 primarily driven by the large-scale wind stress curl generated by the southeast trade wind and the
325 westerlies in the Southern Hemisphere (Beal et al. 2011).

326 In OnlyAT, the role of the Antarctic in intensifying the westerlies and thus the ACC in the
327 Southern Ocean is robust (Fig. 7b2). There is also an anomalous Rossby wave train over the Southern
328 Ocean (Fig. 7b1). The anomalous ACC and Rossby wave train here are much stronger than those in
329 OnlyTP in terms of magnitude. Due to the southward migration of the westerlies (Fig. 6a), the
330 Agulhas leakage is also enhanced by about 1-2 Sv, indirectly reinforcing the AMOC.

331 We want to emphasize again that in OnlyTP, the AMOC is just slightly enhanced even with the
332 help of the stronger Agulhas leakage, due to the lack of strong Ekman pumping in the Southern

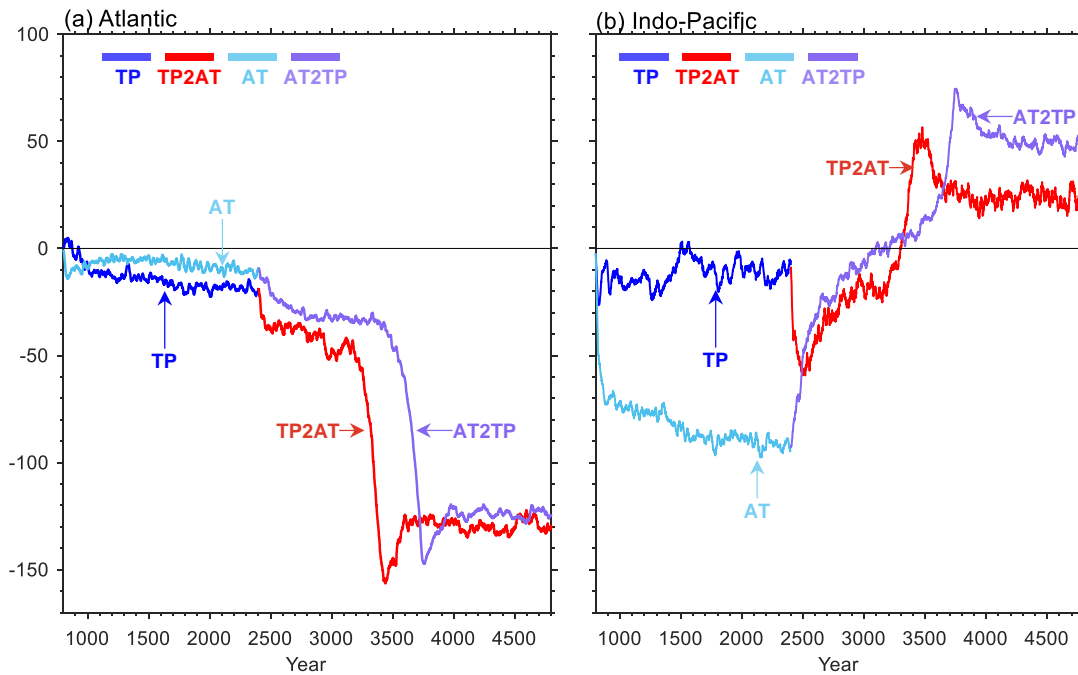
333 Ocean. In OnlyAT, the enhanced Agulhas leakage does not help the AMOC, either, because the
 334 strong Ekman pumping pumps water mainly from the South Pacific. When the TP and Antarctic
 335 coexist, the Agulhas leakage can really contribute to the formation of the AMOC, which is estimated
 336 to be 2-3 Sv based on the TP2AT and AT2TP experiments (Figs. 7c2, d2).



337
 338 FIG. 7. Changes in (left panels) surface wind (vector; units: m/s) and sea-level pressure (shading; units: hPa)
 339 and (right panels) the barotropic streamfunction (units: Sv) in (a) OnlyTP, (b) OnlyAT, (c) TP2AT, and (d)
 340 AT2TP, with respect to Flat. In the left panels, all values are obtained by subtracting their corresponding zonal
 341 mean values; positive (negative) sea-level pressure represents anomalous high (low). In right panels, positive
 342 (negative) barotropic streamfunction represents clockwise (anticlockwise) flow. Note that the scales in (a1) -
 343 (a2) are different from those used in the other panels.

344
 345 When either the TP or Antarctic is present in isolation, the southward mass transport across 30°S
 346 in the South Atlantic is very weak, suggesting a limited AMOC (Fig. 8a). However, a significant
 347 intensification in southward water mass transport within the Atlantic becomes evident only when both

348 topographies are present simultaneously (Fig. 8a), thereby supporting a vigorous AMOC. In the Indo-
 349 Pacific region, the strength of thermohaline circulation is noticeably greater when influenced by the
 350 Antarctic alone, as opposed to the effect of the TP alone (Fig. 8b). This underscores the fact that the
 351 TP's presence disrupts the PMOC. With the concurrent presence of both the TP and Antarctic
 352 topography, the results show a strong northward water mass transport in the Indo-Pacific basin (Fig.
 353 8b), indicating the collapse of the PMOC. The meridional water mass transports are calculated by
 354 integrating the meridional velocity zonally over the depth range of 2000-3000 m across 30°S in the
 355 Atlantic and Indo-Pacific basins.



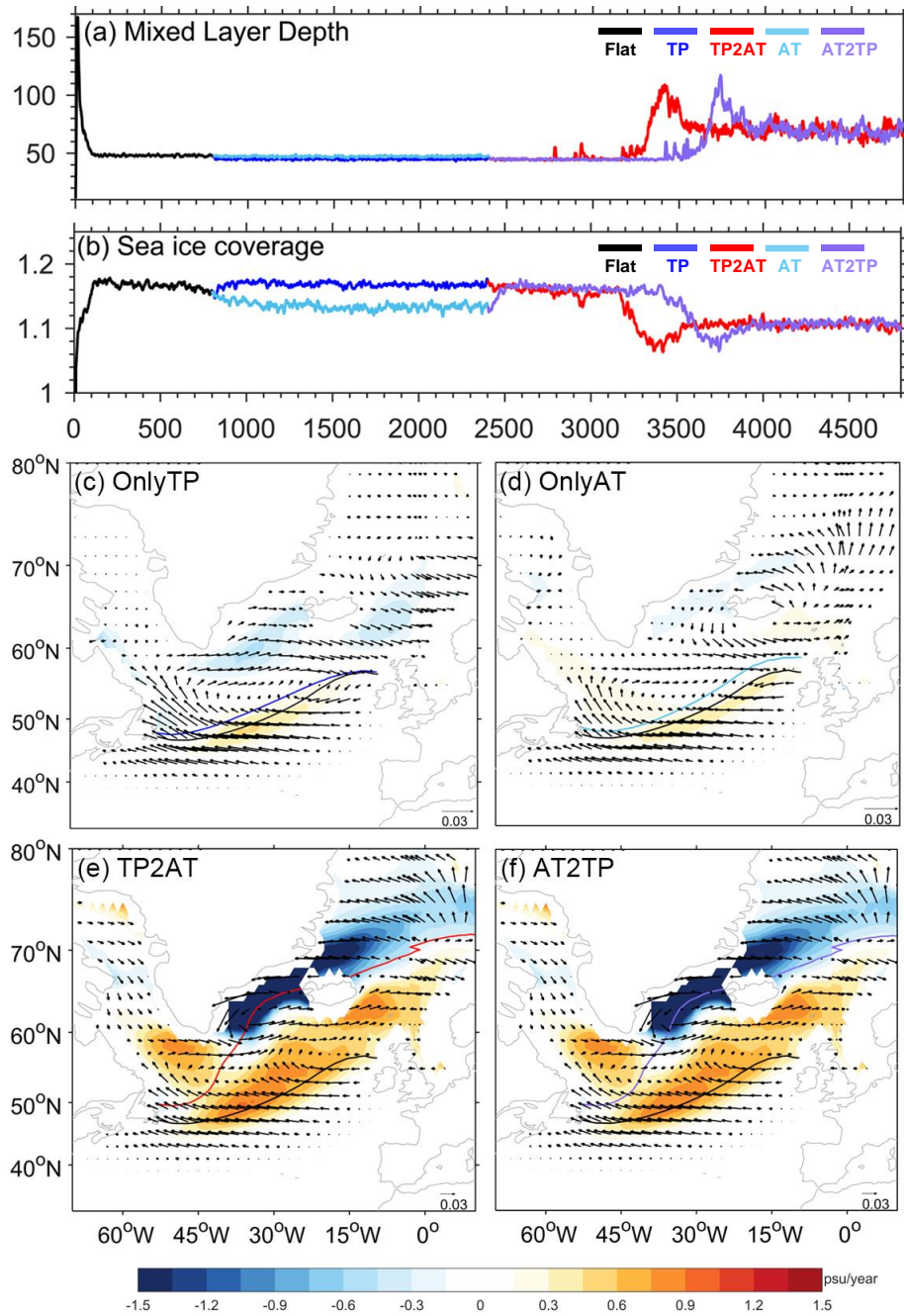
356
 357 FIG. 8. Meridional mass transports across 30°S in (a) the Atlantic and (b) Indo-Pacific. The transport is
 358 calculated by integrating the meridional velocity over the depth range of 2000-3000 m along 30°S in the
 359 respective basin. Positive value represents northward transport, and vice versa. Blue, red, light blue, and purple
 360 lines represent OnlyTP, TP2AT, OnlyAT, and AT2TP, respectively.

361
 362 *e. Positive feedback in the subpolar North Atlantic*

363 With the increased SSS in the North Atlantic, coupled with enhanced Agulhas leakage and
 364 stronger Ekman pumping in the Southern Ocean, the AMOC develops gradually during year 2400-
 365 3200 in TP2AT and year 2400-3600 in AT2TP. A sudden increase in the AMOC strength during its
 366 evolution results from a positive feedback mechanism involving sea ice after year 3200 in TP2AT,

367 and it happens after year 3600 in AT2TP. As the AMOC strengthens, sea ice retreats northward,
368 which in turn diminishes freshwater input into the North Atlantic, enhancing the NADW formation.
369 The MLD over the North Atlantic deepens, and the AMOC develops further. This positive feedback
370 between the AMOC and sea ice leads to rapid changes in both. After year 3200 in TP2AT and 3400 in
371 AT2TP, the AMOC reaches its maximum, and correspondingly, sea ice reaches its minimum within
372 approximately 200 years. The rapid MLD change is consistent with this feedback process as
373 evidenced in Fig. 9a. This positive feedback between the AMOC and sea ice has been reported in
374 numerous previous studies (e.g., Brady and Otto-Bliesner 2011; Yang and Wen. 2020).

375 Apart from the temporal evolution of sea ice, the spatial pattern of virtual salt flux change in the
376 subpolar North Atlantic also supports this mechanism. Compared to the Flat scenario, the virtual salt
377 flux resulting from sea-ice formation or melting in the North Atlantic is markedly elevated in TP2AT
378 and AT2TP (Figs. 9e, f). The positive virtual salt flux signifies a net loss of freshwater from the North
379 Atlantic, accompanied by the northward retreat of sea ice, which is denoted by the location of sea-ice
380 margin. The resulting SSS increase in the North Atlantic is accompanied by a deepening of the MLD
381 in that region (Fig. 4), which ultimately contributes to the strengthening of the AMOC. In OnlyTP
382 and OnlyAT, the sea ice changes are minimal (Figs. 9c, d).



383

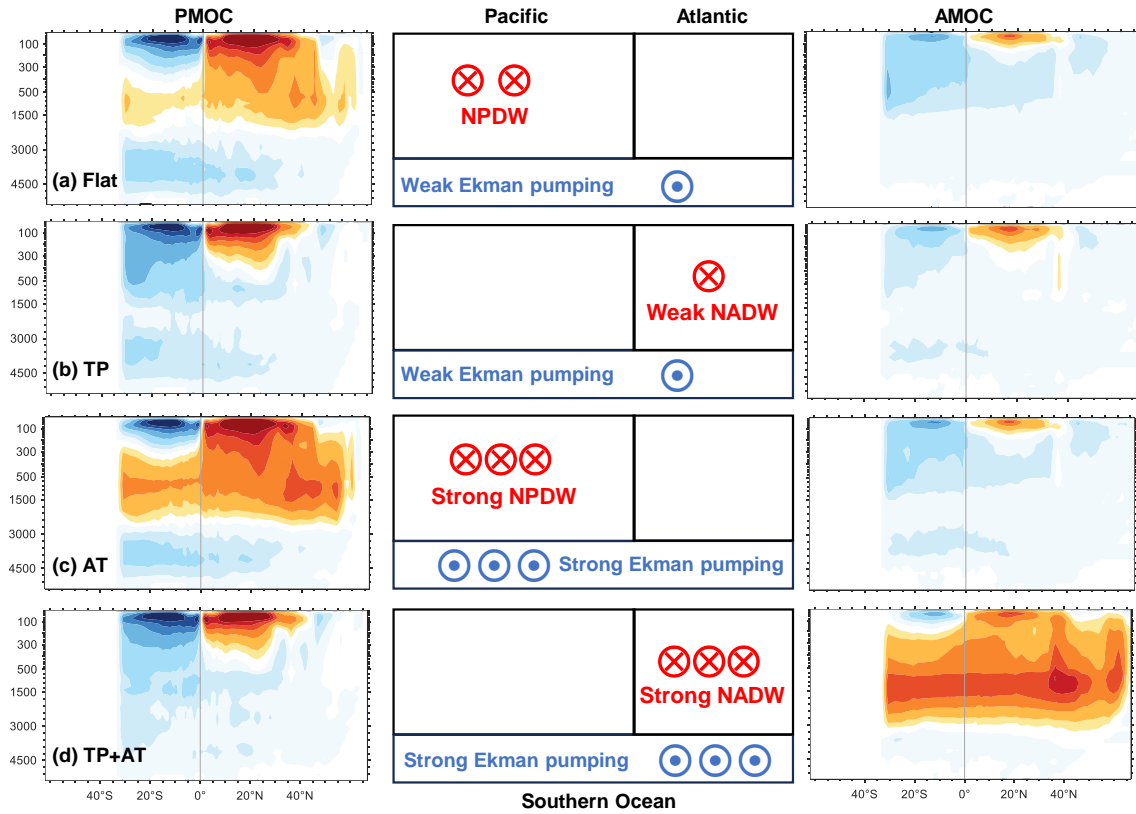
384 FIG. 9. Temporal evolution of (a) March MLD (units: m) and (b) sea-ice coverage (units: 10^6 km^2) in the
 385 Arctic. March MLD is averaged over $40^\circ\text{--}65^\circ\text{N}$ and $20^\circ\text{--}60^\circ\text{W}$. The sea-ice cover is annual averaged. (c)-(f)
 386 Quasi-equilibrium change in virtual salt flux due to sea-ice formation or melting (shading; units: psu/year), and
 387 sea-ice velocity (vector; units: cm/s), with respect to Flat, in OnlyTP, OnlyAT, TP2AT, and AT2TP,
 388 respectively. These changes are annual averaged. Positive (negative) virtual salt flux indicates loss (gain) of
 389 freshwater in the ocean. The sea-ice margin is defined by the 15% sea-ice fraction and plotted as curves, with
 390 the black curve representing that in Flat.

391

392 5. Summary and discussion

393 In this study, we utilized four topographical experiments (OnlyTP, OnlyAT, TP2AT, AT2TP) and
394 two reference experiments (Flat, Real) to investigate the combined effect of the TP and Antarctica on
395 the formation of the AMOC. The results show that it is the combined influence of the TP and the
396 Antarctic orography that maintains the modern day AMOC at its current strength. The presence of the
397 TP is the key for the termination of the PMOC. The fundamental process is the orographic alteration
398 of the atmospheric water cycle that distribute net freshwater fluxes across the world's oceans. It is the
399 current regime of the atmospheric water cycle that enables the high salinity of the northern North
400 Atlantic and the low salinity of sea water within the North Pacific. The presence of the Antarctic has
401 an important role by enhancing southward water mass transport at depth in the South Atlantic and
402 Agulhas leakage south of Africa. The existence of the TP alone, without the Antarctica, is insufficient
403 for the full establishment of the AMOC, underscoring the indispensable role of both topographical
404 features in the dynamics of Earth's climate system. A schematic summary is presented in Fig. 10.

405 The role of the TP is to suppress the NPDW formation, and to provide a favorable condition for
406 the NADW formation, through changing the hydrological pattern in the Northern Hemisphere. The
407 role of the Antarctic orography is to intensify the southward transport of seawater in the intermediate-
408 deep ocean, through enhancing the Ekman pumping in the Southern Ocean. Nonetheless, it does not
409 specify the origin of the southward-flowing water in terms of which ocean basin it comes from. With
410 the addition of the Antarctic to the TP, the NADW formation can literally develop. We stress that the
411 quasi-equilibrium response in these topography experiments does not depend on the manner in which
412 order the topography is introduced; however, the transient response does. The slower evolution of the
413 AMOC in AT2TP than that in TP2AT is mainly due to the difference in the location of deep-water
414 formation.



415

416 FIG. 10. Schematic diagram showing the combined role of the TP and Antarctica. The left (right) panels show
 417 the quasi-equilibrium pattern of the PMOC (AMOC) in respective experiments. The middle panels show
 418 schematically the deep-water formation in the North Pacific and North Atlantic, and the Ekman pumping in the
 419 Southern Ocean. “⊗” represents downward motion of seawater, while “⊙” represents Ekman upwelling.

420

421 The results presented here have important implications for our fundamental understanding of the
 422 AMOC mechanisms and its potential role in paleoclimate. The TP uplift span a wide geological
 423 timescale, from its initial uplift around 40 Ma to its mature state around 8 Ma (Chung et al. 1998;
 424 Spicer et al. 2003), which may have played a role in the initial development of Antarctic ice-sheet
 425 around 34 Ma (Bo et al. 2009), the retreat of the continental ice-sheets during 16-10 Ma, and the
 426 development of Arctic sea-ice around 2~3 Ma (Polyak et al. 2010), shaping the climate from the
 427 Oligocene to Pliocene (Li et al. 2019). The gradual TP uplift led to deflection of the atmospheric jet
 428 stream, intensified monsoonal circulation and increased rainfall over the Eurasian continent, and
 429 ultimately restructured the global hydrological cycle and provided favorable conditions for the
 430 NADW formation (Ruddiman and Kutzbach 1989; Raymo and Ruddiman 1992; Wu et al. 2022).

431 Our experiments here explored how the TP and Antarctica influence global ocean circulations. To
432 isolate these effects, we maintain the modern-day configuration of bathymetry, continental layout,
433 greenhouse gas concentration, incident solar radiation, and orbital parameters in our experimental
434 design. Consequently, the findings of this study are subject to these limitations. Additionally, our
435 conclusions might be influenced by the specific model used, including its resolution and river-runoff
436 magnitudes. As discussed in the Introduction, a sensitivity experiment removing the Rocky
437 Mountains, conducted by GFDL, shows that the PMOC is significantly enhanced (Maroon. 2016),
438 which is not as apparent in CESM simulations (Jiang and Yang. 2021). It is important to note that we
439 did not dynamically simulate the Antarctic glaciation. Our use of the modern-day land-sea
440 distribution and ocean gateways could potentially overstate the TP's impact on the formation of the
441 AMOC. Significant oceanic and climatic shifts, such as the closure of the Tethys Seaway, the
442 formation of the Isthmus of Panama, and the opening of the Bering Strait, all post-date the TP's uplift
443 (Zhang et al. 2022) and have profound implications for ocean circulations and the NADW formation
444 (Schneider and Schmittner 2006; Hamon and Sepulchre 2013; Hu et al. 2015). Moreover, our
445 experiments are set against a backdrop of preindustrial conditions with a stable CO₂ level,
446 disregarding the influence of chemical erosion in rapidly uplifting regions on atmospheric CO₂. The
447 uplift of the TP might have led to reduced atmospheric CO₂ levels, further encouraging the NADW
448 formation through the expansion of continental ice sheets in the Northern Hemisphere (Raymo and
449 Ruddiman 1992). A comprehensive understanding of the uplift's impact on global climate
450 necessitates a quantitative insight into the long-term carbon cycle. Given the complex interplay of
451 factors influencing long-term climate evolution, their contributions need to be further examined.

452 Despite these caveats, we want to underscore the significant role that the TP and Antarctica may
453 have played in the evolution of global thermohaline circulations. This study highlights the importance
454 of coupling among the oceans, the atmosphere and the large-scale orography in shaping our climate.
455 We hope these findings can help to better understand and interpret past and future climate states and
456 transitions.

457 *Acknowledgement:* This research is jointly supported by the NSF of China (Nos. 42288101,
458 42230403, and 41725021) and by the foundation at the Shanghai Frontiers Science Centre of
459 Atmosphere-Ocean Interaction of Fudan University.

460 *Data Availability Statement:*

461 Datasets from this research can be obtained at <https://corp.fudan.edu.cn/Data4Paper.htm>.

References

- 462
463 Beal, L., De Ruijter, W., Biastoch, A. *et al*, 2011: On the role of the Agulhas system in ocean
464 circulation and climate. *Nature*, **472**, 429–436. <https://doi.org/10.1038/nature09983>.
- 465 Bo, S., and Coauthors, 2009: The Gamburtsev mountains and the origin and early evolution of the
466 Antarctic Ice Sheet. *Nature*, **459**, 690–693, <https://doi.org/10.1038/nature08024>.
- 467 Bryden, H. L., 2021: Wind-driven and buoyancy-driven circulation in the subtropical North Atlantic
468 Ocean. *Proceedings of the Royal Society A*, **477**, 2256, <https://doi.org/10.1098/rspa.2021.0172>.
- 469 Buizert, C., and A. Schmittner, 2015: Southern Ocean control of glacial AMOC stability and
470 Dansgaard-Oeschger interstadial duration. *Paleoceanography*, **30**, 1595–1612,
471 <https://doi.org/10.1002/2015PA002795>.
- 472 Chung, S.-L., C.-H. Lo, T.-Y. Lee, Y. Zhang, Y. Xie, X. Li, K.-L. Wang, and P.-L. Wang, 1998:
473 Diachronous uplift of the Tibetan plateau starting 40 Myr ago. *Nature*, **394**, 769–773,
474 <https://doi.org/10.1038/29511>.
- 475 Dekker, M. M., A. S. Von Der Heydt, and H. A. Dijkstra, 2018: Cascading transitions in the climate
476 system. *Earth Syst. Dynam.*, **9**, 1243–1260, <https://doi.org/10.5194/esd-9-1243-2018>.
- 477 Delworth, T. L., and F. Zeng, 2008: Simulated impact of altered Southern Hemisphere winds on the
478 Atlantic Meridional Overturning Circulation. *Geophys. Res. Lett.*, **35**, L20708,
479 <https://doi.org/10.1029/2008GL035166>.
- 480 Ditlevsen, P., and S. Ditlevsen, 2023: Warning of a forthcoming collapse of the Atlantic meridional
481 overturning circulation. *Nat Commun*, **14**, 4254, <https://doi.org/10.1038/s41467-023-39810-w>.
- 482 Fallah, B., U. Cubasch, K. Prömmel, and Coauthors, 2016: A numerical model study on the behavior
483 of Asian summer monsoon and AMOC due to orographic forcing of the Tibetan Plateau. *Clim.*
484 *Dyn.*, **47**, 1485–1495, <https://doi.org/10.1007/s00382-015-2914-5>.
- 485 Ferreira, D., and Coauthors, 2018: Atlantic-Pacific Asymmetry in Deep Water Formation. *Annu. Rev.*
486 *Earth Planet. Sci.*, **46**, 327–352, <https://doi.org/10.1146/annurev-earth-082517-010045>.
- 487 Hamon, N., and P. Sepulchre, V. Lefebvre, and G. Ramstein, 2013: The role of eastern Tethys seaway
488 closure in the Middle Miocene Climatic Transition (ca. 14 Ma). *Clim Past*, **9**, 2687–2702,
489 <https://doi.org/10.5194/cp-9-2687-2013>.
- 490 Hu, A., G. A. Meehl, W. Han, et al., 2015: Effects of the Bering Strait closure on AMOC and global
491 climate under different background climates. *Progress in Oceanography*, **132**, 174–196,
492 <https://doi.org/10.1016/j.pocean.2014.02.004>.

- 493 Hurrell, James W., Holland, M. M. *et al*, 2013: *The Community Earth System Model: A Framework*
494 *for Collaborative Research*. United States. <https://doi.org/10.1175/bams-d-12-00121.1>.
- 495 Ivanova, E., 2009: *The Global Thermohaline Paleocirculation*. Springer Netherlands, ISBN 978-90-
496 481-2414-5.
- 497 Jackson, L.C., Biastoch, A., Buckley, M.W. *et al*, 2022: The evolution of the North Atlantic
498 Meridional Overturning Circulation since 1980. *Nat Rev Earth Environ*, **3**, 241–25,
499 <https://doi.org/10.1038/s43017-022-00263-2>
- 500 Jiang, R., and H. Yang, 2021: Roles of the Rocky Mountains in the Atlantic and Pacific Meridional
501 Overturning Circulations. *J. Climate*, **34**, 6691–6703, <https://doi.org/10.1175/JCLI-D-20-0819.1>.
- 502 Kuhlbrodt, T., A. Griesel, M. Montoya, A. Levermann, M. Hofmann, and S. Rahmstorf, 2007: On the
503 driving processes of the Atlantic meridional overturning circulation. *Reviews of Geophysics*, **45**,
504 RG2001, <https://doi.org/10.1029/2004RG000166>.
- 505 Large, W. G., G. Danabasoglu, S. C. Doney, and J. C. McWilliams, 1997: Sensitivity to surface
506 forcing and boundary layer mixing in a global ocean model: Annual-mean climatology. *J. Phys.*
507 *Oceanogr.*, **27**, 2418–2447.
- 508 Leutert, T. J., A. Auderset, A. Martínez-García, S. Modestou, and A. N. Meckler, 2020: Coupled
509 Southern Ocean cooling and Antarctic ice sheet expansion during the middle Miocene. *Nat.*
510 *Geosci.*, **13**, 634–639, <https://doi.org/10.1038/s41561-020-0623-0>.
- 511 Li, X., and Coauthors, 2019: Late Miocene–Pliocene climate evolution recorded by the red clay cover
512 on the Xiaoshuizi planation surface, NE Tibetan Plateau. *Clim. Past*, **15**, 405–421,
513 <https://doi.org/10.5194/cp-15-405-2019>.
- 514 Liu, Y., Q. Bao, A. Duan, Z. Qian, and G. Wu, 2007: Recent progress in the impact of the Tibetan
515 Plateau on climate in China. *Adv. Atmos. Sci.*, **24**, 1060–1076, [https://doi.org/10.1007/s00376-](https://doi.org/10.1007/s00376-007-1060-3)
516 [007-1060-3](https://doi.org/10.1007/s00376-007-1060-3).
- 517 Lu, M., B. Huang, Z. Li, S. Yang, and Z. Wang, 2019: Role of Atlantic air–sea interaction in
518 modulating the effect of Tibetan Plateau heating on the upstream climate over Afro-Eurasia–
519 Atlantic regions. *Clim Dyn*, **53**, 509–519, <https://doi.org/10.1007/s00382-018-4595-3>.
- 520 Maffre, P., J.-B. Ladant, Y. Donnadieu, P. Sepulchre, and Y. Goddérís, 2018: The influence of
521 orography on modern ocean circulation. *Clim Dyn*, **50**, 1277–1289,
522 <https://doi.org/10.1007/s00382-017-3683-0>.
- 523 Maroon, E. A., 2016: The roles of land and orography on precipitation and ocean circulation in global
524 climate models. Ph.D. thesis, University of Washington, 155 pp.

- 525 Marzocchi, A., and M. F. Jansen, Connecting Antarctic Sea ice to deep-ocean circulation in modern
526 and glacial climate simulations. *Geophys. Res. Lett.*, **44**, 6286–6295,
527 <https://doi.org/10.1002/2017GL073936>.
- 528 Meehl, G. A., A. Hu, J. M. Arblaster, J. Fasullo, and K. E. Trenberth, 2013: Externally Forced and
529 Internally Generated Decadal Climate Variability Associated with the Interdecadal Pacific
530 Oscillation. *Journal of Climate*, **26**, 7298–7310, <https://doi.org/10.1175/JCLI-D-12-00548.1>.
- 531 Patara, L., and C. W. Böning, 2014: Abyssal ocean warming around Antarctica strengthens the
532 Atlantic overturning circulation. *Geophys. Res. Lett.*, **41**, 3972–3978,
533 <https://doi.org/10.1002/2014GL059923>.
- 534 Pearson, P., Foster, G. & Wade, B. Atmospheric carbon dioxide through the Eocene–Oligocene
535 climate transition. *Nature*, **461**, 1110–1113 (2009). <https://doi.org/10.1038/nature08447>.
- 536 Polyak, L., and Coauthors, 2010: History of sea ice in the Arctic. *Quaternary Science Reviews*, **29**,
537 1757–1778, <https://doi.org/10.1016/j.quascirev.2010.02.010>.
- 538 Rahmstorf, S., Thermohaline circulation: The current climate. *Nature*, **421**, 699 (2003).
539 <https://doi.org/10.1038/421699a>
- 540 Ruddiman, W. F., and J. E. Kutzbach, 1989: Forcing of late Cenozoic northern hemisphere climate by
541 plateau uplift in southern Asia and the American West. *J. Geophys. Res.*, **94**, 18409–18427,
542 <https://doi.org/10.1029/JD094iD15p18409>.
- 543 Raymo, M. E., and W. F. Ruddiman, 1992: Tectonic forcing of late Cenozoic climate. *Nature*, **359**,
544 117–122, <https://doi.org/10.1038/359117a0>.
- 545 Schmittner, A., T. A. M. Silva, K. Fraedrich, E. Kirk, and F. Lunkeit, 2011: Effects of Mountains and
546 Ice Sheets on Global Ocean Circulation. *J. Climate*, **24**, 2814–2829,
547 <https://doi.org/10.1175/2010JCLI3982.1>.
- 548 Schneider, B., and A. Schmittner, 2006: Simulating the impact of the Panamanian seaway closure on
549 ocean circulation, marine productivity and nutrient cycling. *Earth and Planetary Science Letters*,
550 **246**, 367–380, <https://doi.org/10.1016/j.epsl.2006.04.028>.
- 551 Singh, H. K. A., C. M. Bitz, and D. M. W. Frierson, 2016: The Global Climate Response to Lowering
552 Surface Orography of Antarctica and the Importance of Atmosphere–Ocean Coupling. *J.*
553 *Climate*, **29**, 4137–4153, <https://doi.org/10.1175/JCLI-D-15-0442.1>.
- 554 Sinha, B., Blaker, A. T., Hirschi, J. J.-M., Bonham, S., Brand, M., Josey, S., Smith, R. S., and
555 Marotzke, J., 2012: Mountain ranges favour vigorous Atlantic meridional overturning, *Geophys.*
556 *Res. Lett.*, **39**, L02705, <https://doi.org/10.1029/2011GL050485>.

- 557 Song, H., A. J. Miller, B. D. Cornuelle, and E. Di Lorenzo, 2011: Changes in upwelling and its water
558 sources in the California Current System driven by different wind forcing. *Dynamics of*
559 *Atmospheres and Oceans*, **52**, 170–191, <https://doi.org/10.1016/j.dynatmoce.2011.03.001>.
- 560 Spicer, R. A., N. B. W. Harris, M. Widdowson, A. B. Herman, S. Guo, P. J. Valdes, J. A. Wolfe, and
561 S. P. Kelley, 2003: Constant elevation of southern Tibet over the past 15 million years. *Nature*,
562 **421**, 622–624, <https://doi.org/10.1038/nature01356>.
- 563 Stouffer, R. J., J. L. Russell, R. L. Beadling, A. J. Broccoli, J. P. Krasting, S. Malyshev, and Z.
564 Naiman, 2022: The Role of Continental Topography in the Present-Day Ocean’s Mean Climate.
565 *J. Climate*, **35**, 1327–1346, <https://doi.org/10.1175/JCLI-D-20-0690.1>.
- 566 Su, B., D. Jiang, R. Zhang, P. Sepulchre, and G. Ramstein, 2018: Difference between the North
567 Atlantic and Pacific meridional overturning circulation in response to the uplift of the Tibetan
568 Plateau. *Clim. Past*, **14**, 751–762, <https://doi.org/10.5194/cp-14-751-2018>.
- 569 Tang, Y., and Coauthors, 2022: Northward Shift of the Northern Hemisphere Westerlies in the Early
570 to Late Miocene and Its Links to Tibetan Uplift. *Geophysical Research Letters*, **49**,
571 e2022GL099311, <https://doi.org/10.1029/2022GL099311>.
- 572 Toggweiler, J. R., 1994: The Ocean’s Overturning Circulation. *Physics Today*, **47**, 45–50,
573 <https://doi.org/10.1063/1.881425>.
- 574 van Westen, R. M., M. Kliphuis, and H. A. Dijkstra, 2024: Physical-based early warming signal
575 shows that AMOC is on tipping course. *Sci. Adv.*, **10**, eadk1189.
- 576 Wang, L., H. Yang, Q. Wen, Y. Liu, and G. Wu, 2023: The Tibetan Plateau’s Far-Reaching Impacts on
577 Arctic and Antarctic Climate: Seasonality and Pathways. *J. Climate*, **36**, 1399–1414,
578 <https://doi.org/10.1175/JCLI-D-22-0175.1>.
- 579 Weijer, W., 2002: Response of the Atlantic overturning circulation to South Atlantic sources of
580 buoyancy. *Global and Planetary Change*, **34**, 293–311, [https://doi.org/10.1016/S0921-](https://doi.org/10.1016/S0921-8181(02)00121-2)
581 [8181\(02\)00121-2](https://doi.org/10.1016/S0921-8181(02)00121-2).
- 582 Wen, Q., C. Zhu, Z. Han, Z. Liu, and H. Yang, 2021: Can the Topography of Tibetan Plateau Affect
583 the Antarctic Bottom Water? *Geophysical Research Letters*, **48**,
584 <https://doi.org/10.1029/2021GL092448>.
- 585 —, H. Yang, K. Yang, G. Li, Z. Liu, and J. Liu, 2022: Possible Thermal Effect of Tibetan Plateau
586 on the Atlantic Meridional Overturning Circulation. *Geophysical Research Letters*, **49**,
587 <https://doi.org/10.1029/2021GL095771>.

- 588 Wood, R. A., A. B. Keen, J. F. B. Mitchell, and J. M. Gregory, 1999: Changing spatial structure of the
589 thermohaline circulation in response to atmospheric CO₂ forcing in a climate model. *Nature*,
590 **399**, 572–575, <https://doi.org/10.1038/21170>.
- 591 Wu, F., X. Fang, Y. Yang, et al., 2022: Reorganization of Asian climate in relation to Tibetan Plateau
592 uplift. *Nat Rev Earth Environ*, **3**, 684–700, <https://doi.org/10.1038/s43017-022-00331-7>.
- 593 Yang, H., and Q. Wen, 2020: Investigating the Role of the Tibetan Plateau in the Formation of
594 Atlantic Meridional Overturning Circulation. *J. Climate*, **33**, 3585–3601,
595 <https://doi.org/10.1175/JCLI-D-19-0205.1>.
- 596 Yang, H., R. Jiang, Q. Wen, Y. Liu, G. Wu, and J. Huang, 2024: The role of mountains in shaping the
597 global meridional overturning circulation. *Nat Commun*, **15**, 2602,
598 <https://doi.org/10.1038/s41467-024-46856-x>.
- 599 Zhang, Y., A. M. de Boer, D. J. Lunt, D. K. Hutchinson, et al., 2022: Early Eocene ocean meridional
600 overturning circulation: The roles of atmospheric forcing and strait geometry. *Paleoceanography*
601 *and Paleoclimatology*, **37**, e2021PA004329, <https://doi.org/10.1029/2021PA004329>.
- 602 Zhu, C., Liu, Z, 2020: Weakening Atlantic overturning circulation causes South Atlantic salinity pile-
603 up. *Nat. Clim. Chang.* **10**, 998–100, <https://doi.org/10.1038/s41558-020-0897-7>.